Finite difference solutions of magneto hydrodynamic free convective flow with constant suction and variable thermal conductivity in a Darcy-Forchheimer porous medium

[1]Ime Jimmy Uwanta, [2]Halima Usman*
Department of Mathematics, Usmanu Danfodiyo University, Sokoto, Nigeria

Abstract: *This paper presents the study of the effects of variable thermal conductivity and Darcy-Forchheimer on magnetohydrodynamic free convective flow in a vertical channel in the presence of constant suction. The resulting governing equations are non-dimensionalised, simplified and solved using Crank Nicolson type of finite difference method. To check the accuracy of the numerical solution, steady-state solutions for velocity, temperature and concentration profiles are obtained by using perturbation method. Numerical results for the velocity, temperature and concentration profiles are illustrated graphically while the skin friction, Nusselt number and Sherwood number are tabulated and discussed for some selected controlling thermo physical parameters involved in the problem to show the behavior of the flow transport phenomena. It is found that the velocity and temperature increased due to increase in variable thermal conductivity parameter and there is decrease in concentration due to increase in Darcy-Forchheimer number. It is also observed that the numerical and analytical solutions are found to be in excellent agreement.*

Keywords: *Variable thermal conductivity, Porous medium, Magnetohydrodynamic, Chemical reaction, Darcy-Forchheimer.*

I.   Introduction

There has been a great deal of interest generated in the area of heat and mass transfer of free convective flow in porous medium due to it is numerous applications in a variety of industrial processes as well as in many natural circumstances. The subject of free convective flow in porous media has attracted considerable attention in the last few decades. Examples of such technological applications are ground water flows, thermal insulation engineering, food processing, soil pollution, fibrous insulation, geothermal extraction to name just a few. A comprehensive bibliography concerned with literature on convective flow in porous media can be found in the books of Nield and Bejan [12] and Ingham and Pop [6]. Processes involving heat and mass transfer effect have long been recognized as important principle in chemical processing equipment. The effect of chemical reaction, heat and mass transfer along a wedge with heat source and concentration in the presence of suction or injection have been examine by Kandasamy et al. [7]. Sattar [15] analyzed the effect of free and forced convection boundary layer flow through a porous medium with large suction. Mohammed et al. [11] investigated the effect of similarity solution for MHD flow through vertical porous plate with suction. In most of the studies on hydromagnetic heat transfer, thermal conductivity has been taken as constant. In metallurgical processing, the numerical value of thermal conductivity changes with temperature. Therefore the thermal conductivity is temperature dependent. In order to predict the accuracy of heat and mass transfer flow, mathematical models most consider the variation of thermal conductivity with temperature. Many papers were published with problem of thermal conductivity under different physical and geothermal conditions. Patowary and Dusmata [13] have presented the effects of thermal conductivity of micropolar fluid past a continuously moving plate with suction or injection in presence of magnetic field. Abdou [1] considered the effects of thermal radiation on unsteady boundary layer flow with temperature dependent viscosity and thermal conductivity due to a stretching sheet in porous medium. Similarly, Chiam [3] analyzed the effect of a variable thermal conductivity on the flow and heat transfer from a linearly stretching sheet. In another article, Seddek and Salema [18] have studied the effects of variable viscosity and thermal conductivity on an unsteady two-dimensional laminar flow of a viscous incompressible conducting fluid past a vertical plate taking into account the effect of magnetic field in the presence of variable suction. Gitima [4] presented a numerical model on the effect of thermal radiation on unsteady boundary layer flow with variable viscosity and variable thermal conductivity due to stretching sheet in a porous channel in the presence of magnetic field. Additionally Hossain et al. [5] described the study of natural convection with variable viscosity and thermal conductivity from a vertical wavy cone. Sharma and Singh [19] have presented a theoretical study on the effects of variable thermal conductivity and heat source/sink on MHD flow near a stagnation point on a linearly stretching sheet. Very recently, Uwanta and Murtala [20] investigated the study of heat and mass transfer flow past an infinite vertical plate with variable thermal conductivity. Although considerable work has been reported on heat and mass transfer by free

convection in a porous medium, majority of porous studies have been on Darcy's law which states that the volume-averaged velocity is proportional to the pressure gradient which is valid only for slow flows through porous media with low permeability. However, Darcy's law fails when the velocities and inertial effects are greater. Inertial porous phenomena can be accounted through the addition of a velocity-squared term in the momentum equation and the resulting model is known as Darcy-Forchheimer model Vafai and Tien [21]. The Darcy-Forchheimer model described the effect of inertia as well as viscous forces in porous media. Many investigators have reported work on Darcy and Darcy-Forchheimer. Numerical simulation of chemical reaction and viscous dissipation effects on Darcy-Forchheimer mixed convection in a fluid saturated media has been investigate by Mahdy and Chamkha [10]. Salem [17] has presented the radiation and mass transfer effects in Darcy-Forchheimer mixed convection from a vertical plate embedded in a fluid saturated porous medium. Lai [9] studied mixed convection heat and mass transfer from a vertical wall in a Darcian fluid saturated porous medium. Additionally, Kishan et al. [8] analyzed MHD free convective heat and mass transfer from a vertical surface embedded in a porous medium. A detailed numerical study has been carried out on the natural convection in a porous square cavity with an isoflux and isothermal discrete heater placed at the left wall by Saeid and Pop [16] using Darcy law. Rawat et al. [14] have investigated a theoretical study on free convection MHD micropolar flow, heat and species diffusion between vertical plates enclosing a non-Darcian porous medium with variable thermal conductivity and internal heat generation/absorption effects.

Inspite of all these studies, the aim of this work is to investigate the numerical solutions to the system of equations for magnetohydrodynamic free convective flow past a finite vertical channel with constant suction and thermal conductivity in a porous medium using finite difference method.

II.   Mathematical analysis

Consider an unsteady laminar one-dimensional boundary layer heat and mass transfer flow in an electrically conducting fluid with thermal conductivity, chemical reaction and radiation in a Darcy-Forchheimer porous medium. Fluid suction or injection is imposed at the boundary of the cylinder. The x' - axis is taken along the plate in the vertically upward direction and the y' - axis is taken normal to the plate. A uniform transverse magnetic field B_0 is applied normal to the flow direction. The magnetic Reynolds number is assumed to be small so that the assumed magnetic field can be neglected. It is also assumed that the effects of joule heating and viscous dissipation are neglected and the external electric field due to the effect of charge polarization and the hall effect of MHD are neglected. Under these assumptions, the governing boundary layer equations of continuity, momentum, energy and diffusion equations under Boussinesq's approximations could be written as follows:

$$\frac{\partial v'}{\partial y'} = 0 \tag{1}$$

$$\frac{\partial u'}{\partial t'} - v_0 \frac{\partial u'}{\partial y'} = n \frac{\partial^2 u'}{\partial y'^2} - \left(\frac{S B_0^2}{r} + \frac{b'}{K'} \right) u'^2 - \frac{n}{K'} u' + g b (T' - T_0') + g b^* \left(C' - C_0' \right) \tag{2}$$

$$\frac{\partial T'}{\partial t'} - v_0 \frac{\partial T'}{\partial y'} = \frac{k_0}{r C_p} \frac{\partial}{\partial y'} \left[1 + a(T' - T_0') \right] \frac{\partial T'}{\partial y'} - \frac{1}{r C_p} \frac{\partial q_r}{\partial y'} \tag{3}$$

$$\frac{\partial C'}{\partial t'} - v_0 \frac{\partial C'}{\partial y'} = D \frac{\partial^2 C'}{\partial y'^2} - R^* (C' - C_0') \tag{4}$$

The corresponding initial and boundary conditions are prescribed as follows:

$$t \le 0, \qquad u' = 0, \ T' \to T_w', \ C' \to C_w' \ \text{for all} \ y'$$
$$t > 0, \qquad u' = 0, \ T' = T_w', \ C' = C_w' \ \text{at} \ y' = 0 \tag{5}$$
$$u' = 0, \ T' = T_0, \ C' = C_0 \ \text{at} \ y' = H$$

From continuity equation, it is clear that the suction velocity is either a constant or a function of time. Hence, on integrating equation (1), the suction velocity normal to the plate is assumed in the form,

$$v' = -v_0$$

where v_0 is a scale of suction velocity which is non-zero positive constant. The negative sign indicates that the suction is towards the plate and $v_0 > 0$ corresponds to steady suction velocity normal at the surface.

The fourth and fifth terms on the right hand side of equation (2) denote the thermal and concentration buoyancy effects respectively. The last term of equation (3) represents the radiative heat flux term, while the last term of equation (4) is the chemical reaction term. u' and v' are the Darcian velocity components in the x- and y- directions respectively, t is the time, v is the kinematic viscosity, g is the acceleration due to gravity, β is the coefficient of volume expansion, ρ the density of the fluid, σ is the scalar electrical conductivity, β^* is the volumetric coefficient of expansion with concentration, C_p is the specific heat capacity at constant pressure, K' is the Darcy permeability of the porous medium, b' is the empirical constant, k_0 is the dimensionless thermal conductivity of the ambient fluid, α is a constant depending on the nature of the fluid, R^* is the dimensionless chemical reaction, D is the coefficient of molecular diffusivity, v_0 is the constant suction parameter, q_r is the radiative heat flux in the y- direction, B_0 is the magnetic induction of constant strength. T' and T_0' are the temperature of the fluid inside the thermal boundary layer and the fluid temperature in the free stream respectively, while C' and C_0' are the corresponding concentrations.

To obtain the solutions of equations (2), (3) and (4) subject to the conditions (5) in non-dimensional forms, we introduce the following non-dimensional quantities:

$$u = \frac{u'}{u_0}, t = \frac{t' u_0}{H^2}, y = \frac{y'}{H}, q = \frac{T' - T_0'}{T_w' - T_0'},$$

$$C = \frac{C' - C_0'}{C_w' - C_0'}, \Pr = \frac{u_0 r C_p}{k_0}, Sc = \frac{u_0}{D}, Da = \frac{K' u_0}{H^2 v},$$

$$M = \frac{S B_0^2 H^2}{r u_0}, Gr = \frac{H^2 g b \left(T_w' - T_0'\right)}{u_0^2}, Gc = \frac{H^2 g b^* \left(C_w' - C_0'\right)}{u_0^2}, \tag{6}$$

$$l = a\left(T' - T_0'\right), g = \frac{n_0 H}{u_0}, K_r = \frac{R^* H^2}{u_0}, R = \frac{16 a s_0' H T_0'^3}{k' u_0^2}, Fs = \frac{b' u_0}{H^2 v}$$

Applying these non-dimensionless quantities (6), the set of equations (2), (3), (4), and (5) reduces to the following:

$$\frac{\partial u}{\partial t} - \gamma \frac{\partial u}{\partial y} = \frac{\partial^2 u}{\partial y^2} - \left(M + \frac{Fs}{Da}\right) u^2 - \frac{1}{Da} u + Gr\theta + GcC \tag{7}$$

$$\frac{\partial \theta}{\partial t} - \gamma \frac{\partial \theta}{\partial y} = \frac{\lambda}{\Pr} \left(\frac{\partial \theta}{\partial y}\right)^2 + \frac{1}{\Pr}\left(1 + \lambda\theta\right)\frac{\partial^2 \theta}{\partial y^2} - \frac{1}{\Pr} R\theta \tag{8}$$

$$\frac{\partial C}{\partial t} - \gamma \frac{\partial C}{\partial y} = \frac{1}{Sc}\frac{\partial^2 C}{\partial y^2} - K_r C \tag{9}$$

with the following initial and boundary conditions

$$t \le 0 \quad u = 0, \theta = 0, C = 0, \quad for \ all \ y,$$
$$t > 0 \quad u = 0, \theta = 1, C = 1, \quad at \ y = 0, \tag{10}$$
$$u = 0, \theta = 0, C = 0 \quad at \ y = 1.$$

Where $\Pr$ is the Prandtl number, Sc is the Schmidt number, M is the Magnetic field parameter, Gr is the thermal Grashof number, Gc is the Solutal or mass Grashof number, λ is the variable thermal conductivity, γ is the variable suction parameter, R is the Radiation parameter, K_r is the chemical reaction parameter, Da is the Darcy number, Fs is the Darcy-Forchheimer number, t is the dimensionless time while u and v are dimensionless velocity components in x- and y- directions respectively.

III. Analytical solutions

In order to check the accuracy of the present numerical scheme of this model, there is need to compare numerical solutions with the analytical solutions. Since the governing equations are highly coupled and non-linear, it is, therefore, of interest to reduce the governing equations of the present problem due to its non-linearity into a form that can be solved analytically. At steady state the governing equations of the problem becomes:

$$\frac{\partial^2 u}{\partial y^2} + \gamma \frac{\partial u}{\partial y} - \frac{1}{Da} u + Gr\theta + GcC = 0 \tag{11}$$

$$\frac{\partial^2 \theta}{\partial y^2} + \gamma \Pr \frac{\partial \theta}{\partial y} - R\theta = 0 \tag{12}$$

$$\frac{\partial^2 C}{\partial y^2} + \gamma Sc \frac{\partial C}{\partial y} - K_r ScC = 0 \tag{13}$$

The boundary conditions are

$$u = 0, \ \theta = 1, \ C = 1, \quad at \ y = 0,$$
$$u = 0, \ \theta = 0, \ C = 0 \quad at \ y = 1. \tag{14}$$

To find the approximate solution to equations (11)-(13) subject to equation (14), we employed a regular perturbation method by taking a power series expansion and assume solution of the form:

$$u = u_0(y) + Ru_1(y) + 0(R^2)$$
$$\theta = \theta_0(y) + R\theta_1(y) + 0(R^2) \tag{15}$$
$$C = C_0(y) + RC_1(y) + 0(R^2)$$

Using equation (15) into equations (11)-(14) and equating the coefficient of like powers of R, the solutions to the governing equations are obtained as:

$$u = F_9 e^{s_1 y} + F_{10} e^{s_2 y} + F_{11} + F_{12} e^{-\gamma \Pr y} + F_{13} e^{h_1 y} + F_{14} e^{h_2 y} +$$
$$R\left[F_{15} e^{s_1 y} + F_{16} e^{s_2 y} + F_{17} + F_{18} e^{-\gamma \Pr y} + (F_{19} y + F_{20}) e^{-\gamma \Pr y} \right] \tag{16}$$

$$\theta = F_1 + F_2 e^{-\gamma \Pr y} + R\left[F_3 + F_4 e^{-\gamma \Pr y} + (F_5 - F_6) y e^{-\gamma \Pr y} \right] \tag{17}$$

$$C = F_7 e^{h_1 y} + F_8 e^{h_2 y} \tag{18}$$

IV. Numerical solution procedure

To solve the system of transformed coupled non-linear partial differential equations (7)-(9), under the initial and boundary conditions (10), an implicit finite difference scheme of Crank-Nicolson type which is unconditionally stable Carnahan et al, [2] has been employed. The equivalent finite difference approximations corresponding to equations (7)-(9) are given as follows:

$$\left(\frac{u_{i,j+1} - u_{i,j}}{Dt} \right) - \frac{g}{2Dy} \left(u_{i+1,j} - u_{i-1,j} \right) =$$
$$\frac{1}{2(Dy)^2} \left(u_{i+1,j+1} - 2u_{i,j+1} + u_{i-1,j+1} + u_{i+1,j} - 2u_{i,j} + u_{i-1,j} \right) -$$
$$\left(M + \frac{Fs}{Da} \right) \left(u_{i,j} \right)^2 - \frac{1}{Da} \left(u_{i,j} \right) + Gr \left(q_{i,j} \right) + Gc \left(C_{i,j} \right) \tag{19}$$

$$\left(\frac{q_{i,j+1} - q_{i,j}}{\mathrm{D}t}\right) - \frac{g}{2\mathrm{D}y}\left(q_{i+1,j} - q_{i-1,j}\right) =$$

$$\frac{H}{2\mathrm{Pr}\left(\mathrm{D}y\right)^2}\left(q_{i+1,j+1} - 2q_{i,j+1} + q_{i-1,j+1} + q_{i+1,j} - 2q_{i,j} + q_{i-1,j}\right) + \qquad (20)$$

$$\frac{l}{\mathrm{Pr}\left(\mathrm{D}y\right)^2}\left(q_{i+1,j} - q_{i,j}\right)^2 - \frac{R}{\mathrm{Pr}}\left(q_{i,j}\right)$$

$$\left(\frac{C_{i,j+1} - C_{i,j}}{\mathrm{D}t}\right) - \frac{g}{2\mathrm{D}y}\left(C_{i+1,j} - C_{i-1,j}\right) =$$

$$\frac{1}{2Sc\left(\mathrm{D}y\right)^2}\left(C_{i+1,j+1} - 2C_{i,j+1} + C_{i-1,j+1} + C_{i+1,j} - 2C_{i,j} + C_{i-1,j}\right) - \qquad (21)$$

$$K_r\left(C_{i,j}\right)$$

The initial and boundary conditions take the following forms

$$u_{i,j} = 0, \quad q_{i,j} = 0, \quad C_{i,j} = 0$$

$$u_{0,j} = 0, \quad q_{0,j} = 1, \quad C_{0,j} = 1 \qquad (22)$$

$$u_{H,j} = 0, \quad q_{H,j} = 0, \quad C_{H,j} = 0$$

where H corresponds to 1.

The index i corresponds to space y and j corresponds to time t. Δy and Δt are the mesh sizes along y-direction and time t-direction respectively. The analytical solutions obtained in this work are used to check on the accuracy and effectiveness of the numerical scheme. Computations are carried out for different values of physical parameters involved in the problem.

The skin friction coefficient, Nusselt number and Sherwood number are important physical parameters for this type of boundary layer flow, which respectively are given by:

$$C_f = \left(\frac{\partial u}{\partial y}\right)_{y=0}, \quad Nu = -\left(\frac{\partial \theta}{\partial y}\right)_{y=0}, \quad Sh = \left(\frac{\partial C}{\partial y}\right)_{y=0} \qquad (23)$$

V. Results and discussion

Numerical computations have been carried out for various values of thermo physical parameters involved in this work such as thermal Grashof number (Gr), solutal Grashof number (Gc), Magnetic parameter (M), Darcy number $\left(Da\right)$, suction parameter (γ), radiation parameter (R), chemical reaction parameter (K_r), Darcy-Forchheimer number $\left(Fs\right)$, variable thermal conductivity (λ), Prandtl number (Pr) and Schmidt number (Sc) using an implicit method of Crank-Nicolson type. In order to illustrate the results graphically, the numerical values are plotted in Figs. (1-25). Values of local skin friction C_f, Nusselt number Nu and Sherwood number Sh are presented in Tables 1 and 2 for various values of physical parameters. Solutions are obtained for fluids with Prandtl number (Pr = 0.71, 1.0 and 7.0) corresponding to air, salt water and water respectively. The values of Schmidt number are chosen in such a way as they represent the diffusing chemical species of most common interest in air and are taken for (Sc = 0.22 0.60, 0.78, 2.62) corresponding to hydrogen, water, NH_3 and Propyl benzene respectively. Default values of the physical parameters for velocity, temperature and concentration profiles are specified as follows:

$$Gr = 5.0, Gc = 5.0, M = 2.0, K_r = 1.0, \Pr = 0.71, Sc = 0.22, R = 3.0, Da = 0.01,$$

$$Fs = 3.0, g = 5.0, \ell = 0.05.$$

All graphs therefore correspond to these values unless specifically indicated on the appropriate graphs. The effects of various thermo physical parameters on the fluid velocity are illustrated in Figs.1-11 at time $t = 0.1$. The influence of thermal Grashof number and solutal Grashof number are presented in Figs. 1 and 2. As expected, it is observed that there is a rise in the velocity profiles due to the enhancement of thermal and mass buoyancy force. The velocity distribution increases rapidly near the porous plate and then decrease smoothly to the free stream velocity. Fig. 3 illustrates the effect of magnetic parameter on the velocity profile. It is interesting to note that increase in M leads to decreasing the flow velocity. This is because the presence of magnetic field in an electrically conducting fluid tends to produce a body force, which reduces the velocity of the fluid. Fig. 4 depicts typical velocity distribution across the boundary layer for various values of Darcy number. It is seen that the dimensionless velocity increases with increase in Darcy number. This is due to the fact that larger values of Da parameter correspond to higher permeability porous media, which implies that, less porous fiber resistance to the flow and therefore acceleration in transport. The effect of Darcy-Forchheimer parameter is demonstrated in Fig. 5. It is noticed that an increase in Fs parameter increases the resistance to the flow and so a decrease in the velocity profile. Figs. 6-8 graphically illustrate the behavior of Prandtl number, suction and Schmidt number respectively. It is observed that the momentum boundary layer decreases with the increase in $\Pr$ this is due to the fact that convection current becomes weak and hence results in a decrease in the velocity. Also, it is seen that the velocity decreases with an increase in g parameter. This is because suction parameter decelerates fluid particles through porous wall there by reducing the growth of the fluid boundary layers. Figure 8 illustrates the effect of Sc on the velocity profiles. Clearly, it is observed that the velocity distribution decreases with an increase in Sc. This is due to the fact that as Sc increases, the concentration buoyancy effect decreases yielding a reduction in the velocity profiles. The influence of variable thermal conductivity parameter, radiation parameter and dimensionless time are displayed in Figs. 9-11 respectively. It is observed that as λ and t increases the momentum boundary layer increases, while an increase in radiation parameter obviously decreases the velocity within the boundary layer. This is because larger values of R correspond to an increased dominance of conduction over radiation, thereby decreasing the buoyancy force and the thickness of the momentum boundary layer.

The influences of various thermo physical parameters on the temperature distribution are respectively presented in Figs. 12-17 at time $t = 0.2$. Fig. 12 depicts the behavior of Prandtl number that is inversely proportional to the thermal diffusivity of the working fluid on temperature distribution. It is noticed that the thermal boundary layer decreases with increasing $\Pr$. This is due to the fact that as values of $\Pr$ increases, the thermal diffusivity of the fluid increases which results in a corresponding decrease in the temperature within the fluid. The temperature profile decreases with increasing suction parameter in Fig.13. This is because suction decelerates the fluid properties through porous wall thereby reducing the thermal boundary layer. The effect of variable thermal conductivity parameter on temperature profile is shown in Fig. 14. Here it is observed that the temperature profile decreases with increase in the variable thermal conductivity parameter. Fig. 15 described the influence of radiation parameter on the temperature profile. An increase in R leads to increasing the temperature boundary layer. This is obvious because the effect of radiation is to increase the temperature distribution in the thermal boundary layer. Figs.16 and 17 graphically illustrate the effects of Darcy-Forchheimer parameter and dimensionless time. It is observed that there is no significant change in the temperature profile as Darcy-Forchheimer parameter is increased, but there is a rise in the thermal boundary layer as the time increases.

Figs. 18-21 illustrate the concentration profiles for various values of Schmidt number, chemical reaction parameter, suction parameter and Darcy-Forchheimer parameter respectively at time $t = 0.4$. A decrease in concentration profile with increasing these parameters is observed from these figures. This is due to the fact that an increase of Schmidt number means decrease in molecular diffusivity, while suction parameter stabilizes the boundary layer growth and therefore the concentration profile decreased. The effect of dimensionless time on the concentration profile is presented in Fig. 22. It is seen that the concentration profile increases with increase in the dimensionless time. The validity of the present model has been verified by comparing the numerical solutions and the analytical solutions through Fig. 23-25 for velocity, temperature and concentration profiles respectively.These results are presented to illustrate the accuracy of the numerical solution. It is observed that the agreement between the results is excellent because the curves corresponding to analytical and numerical solutions coincide with one another. This has established confidence in the numerical results reported in this paper.
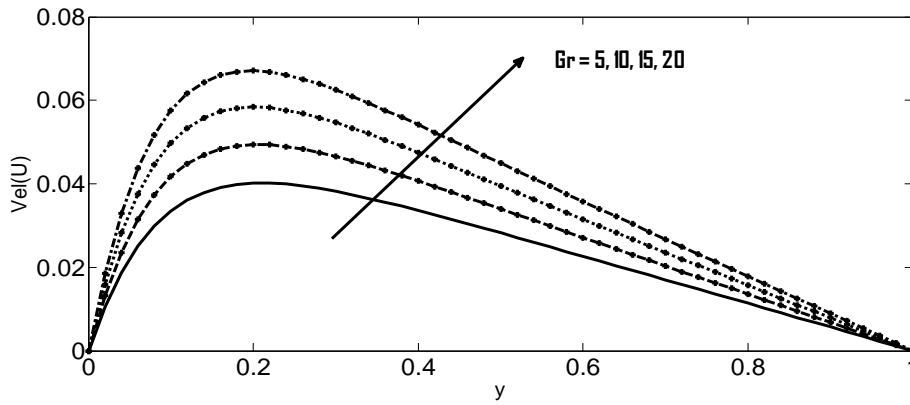
Fig.1. Effect of Gr on the velocity profiles
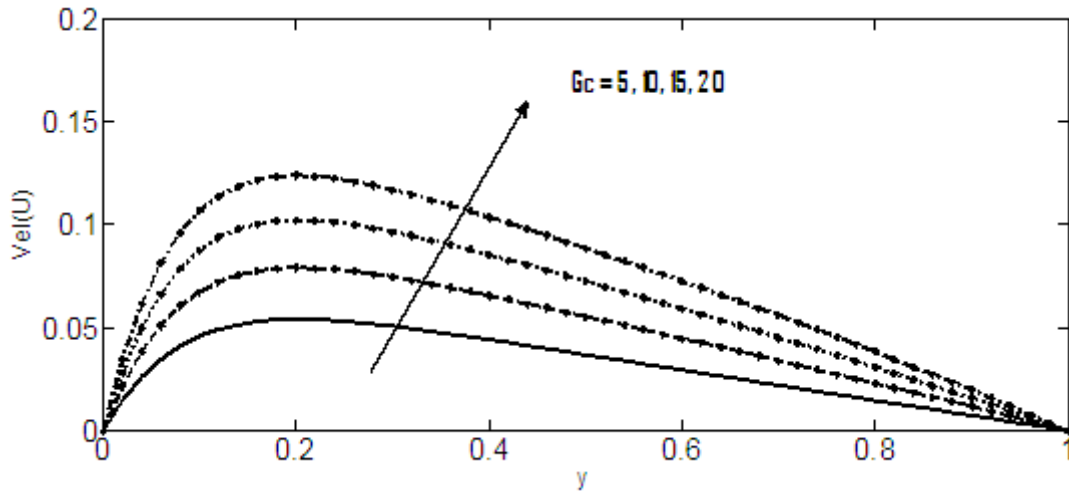
Fig.2. Effect of Gc on the velocity profiles
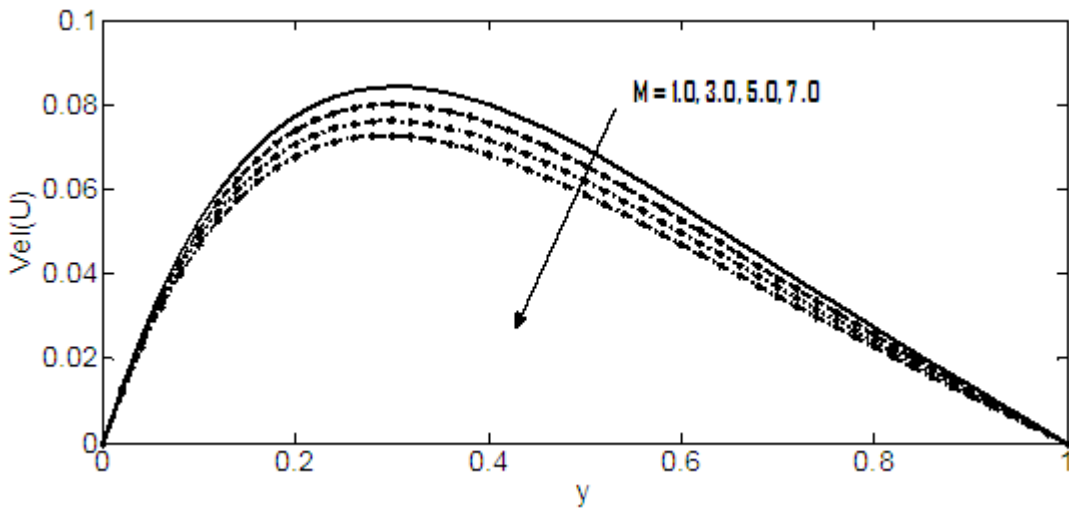
Fig.3. Effect of M on the velocity profiles
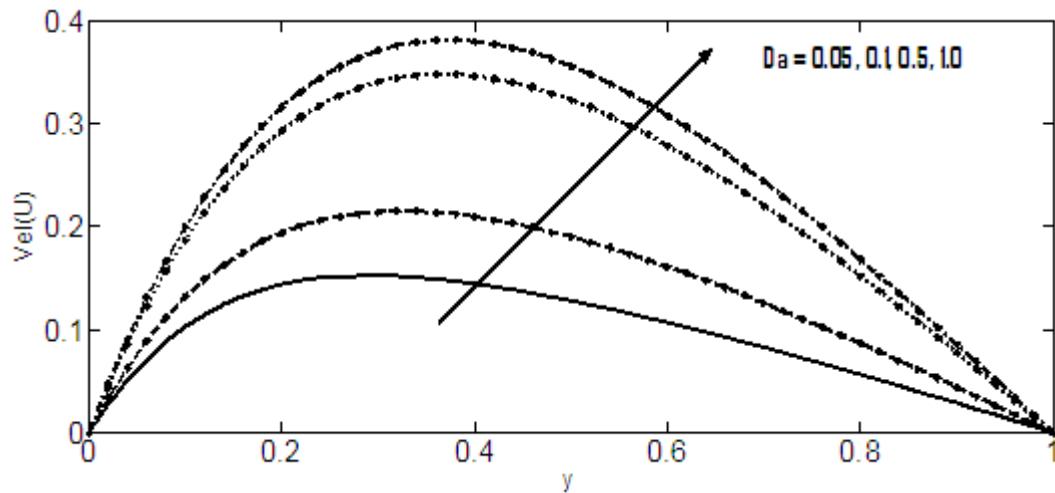
Fig.4. Effect of Da on the velocity profiles
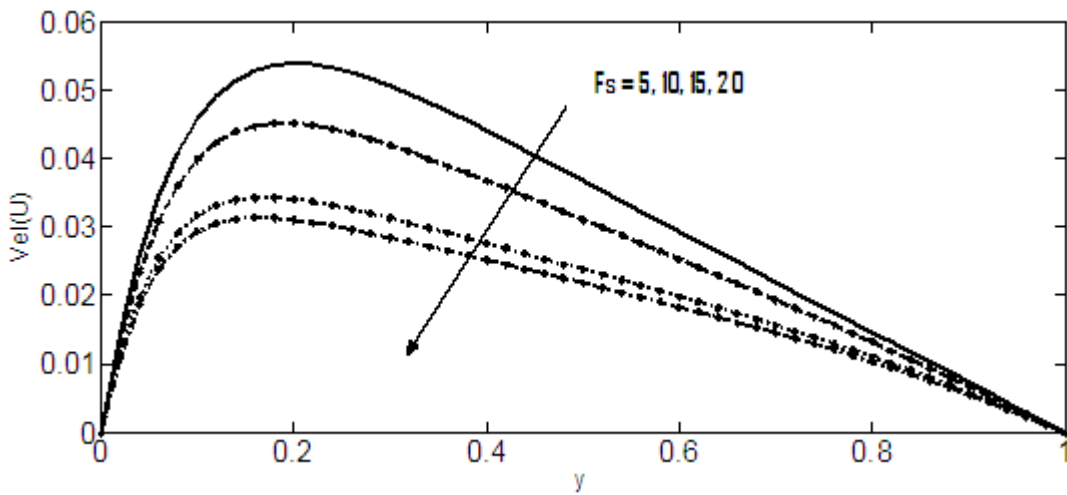
Fig.5. Effect of Fs on the velocity profiles
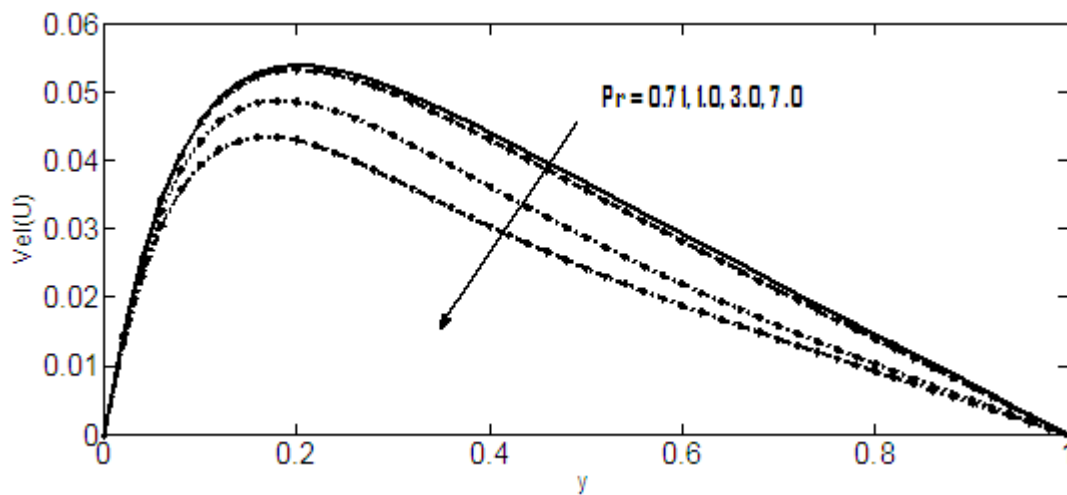
Fig.6. Effect of Pr on the velocity profiles
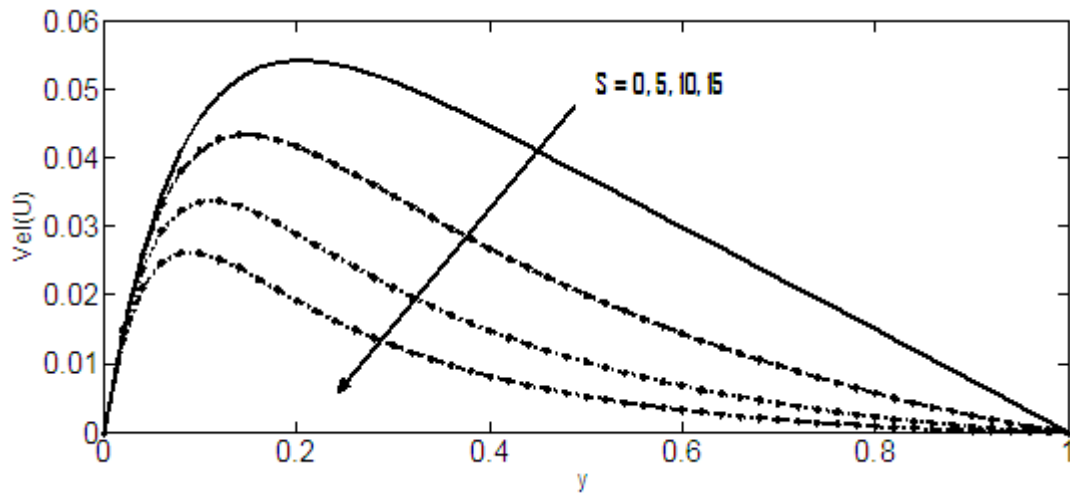
Fig.7. Effect of ($\gamma = S$) on the velocity profiles
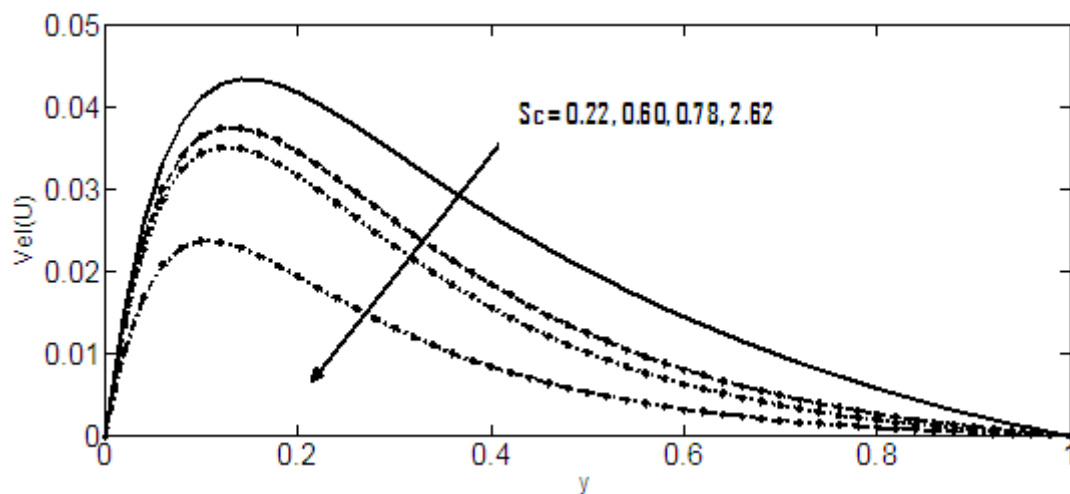
Fig.8. Effect of Sc on the velocity profiles
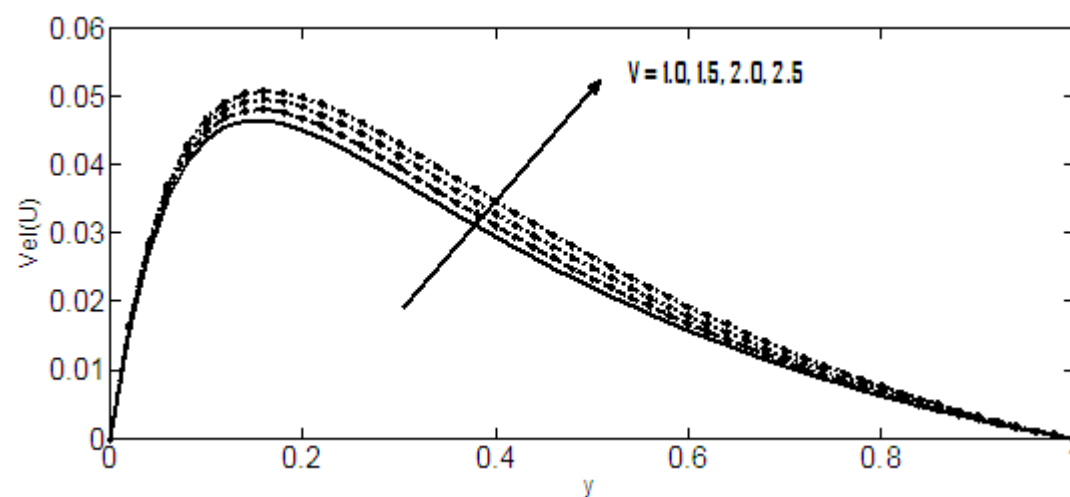
Fig.9. Effect of ($\lambda = V$) on the velocity profiles
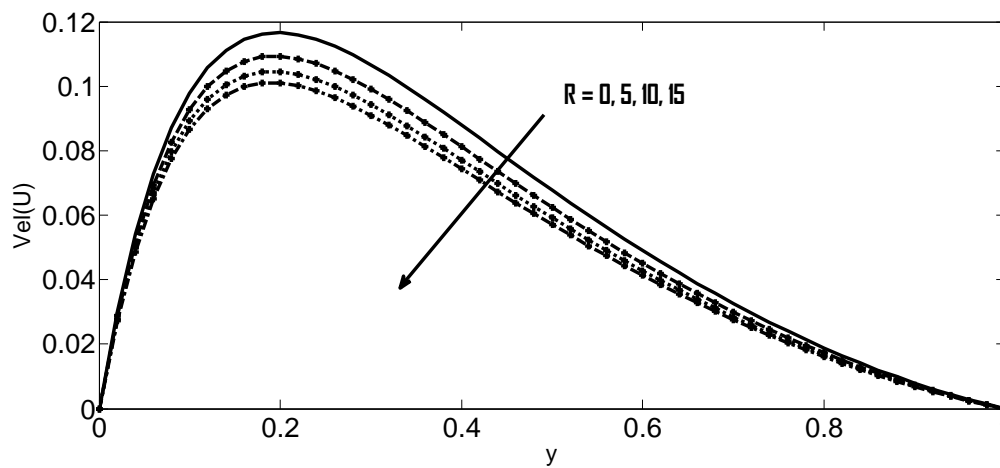
Fig.10. Effect of R on the velocity profiles
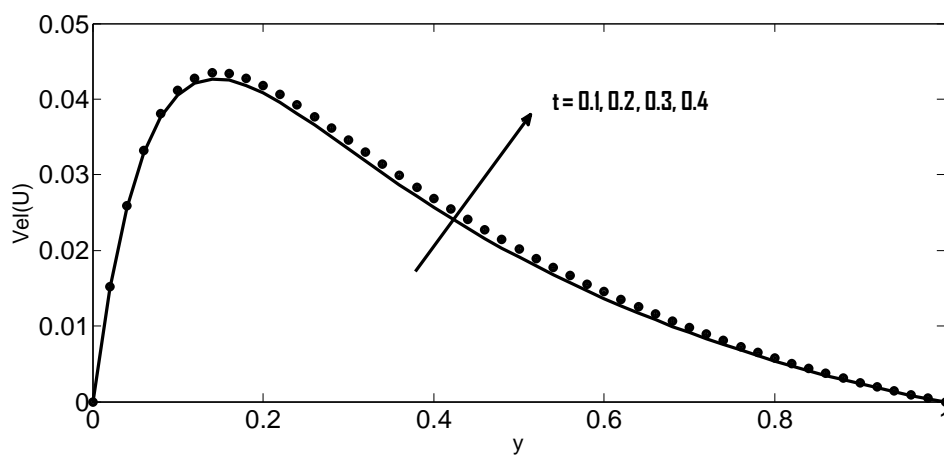
Fig.11. Effect of t on the velocity profiles
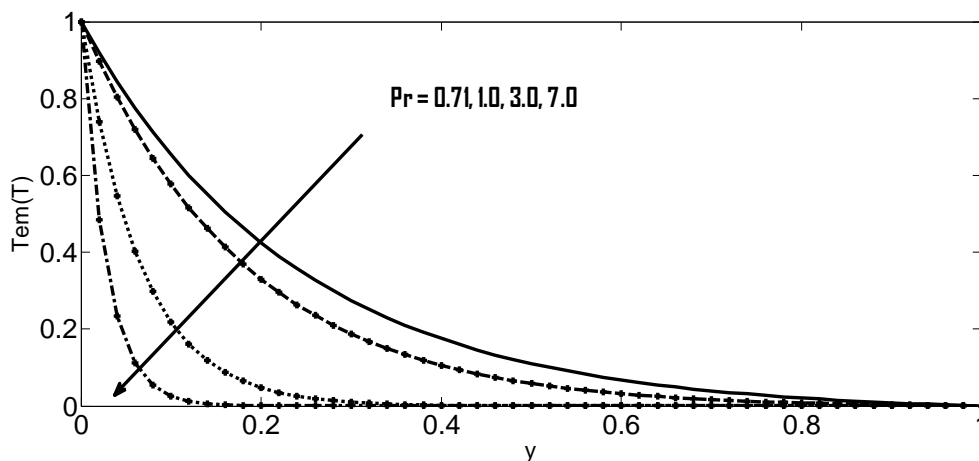
Fig.12. Effect of Pr on the temperature profiles
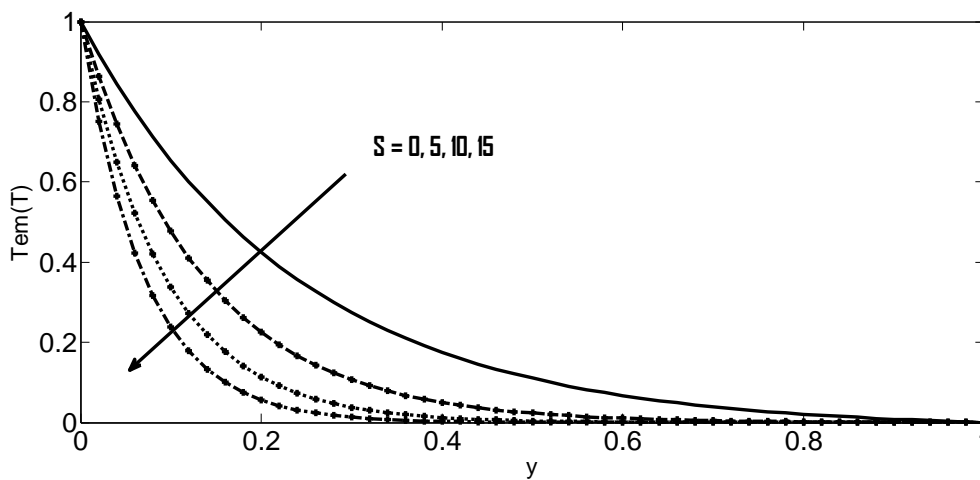
Fig.13. Effect of (γ = S) on the temperature profiles
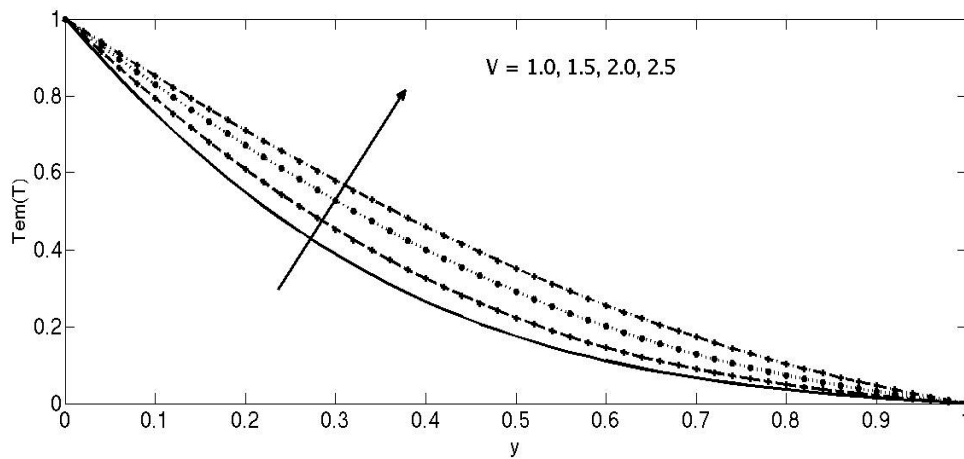
Fig.14. Effect of (λ = V) on the temperature profiles
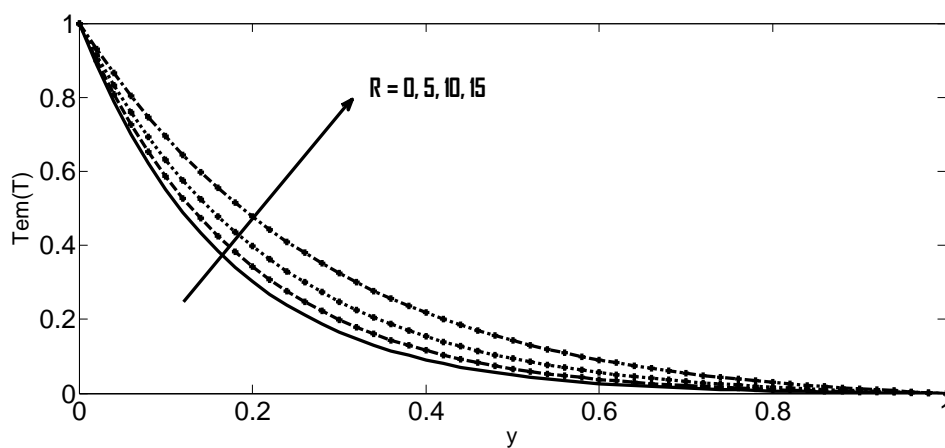
Fig.15. Effect of R on the temperature profiles
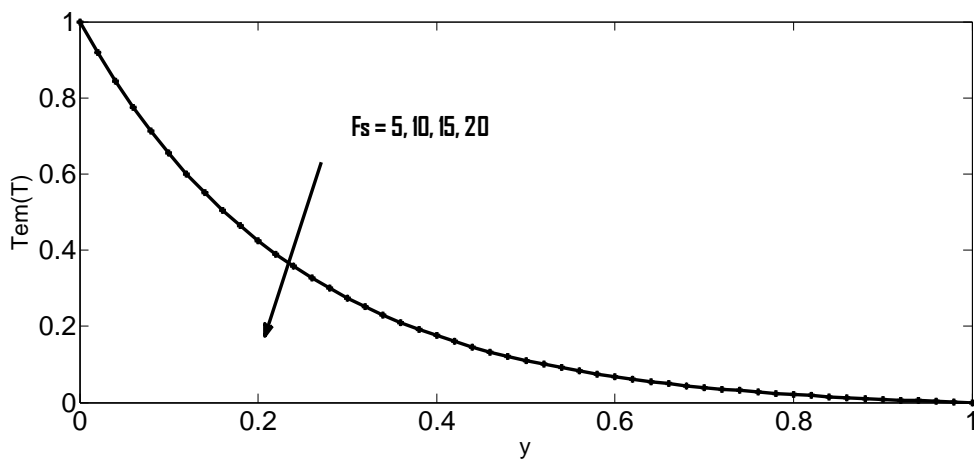
Fig.16. Effect of Fs on the temperature profiles
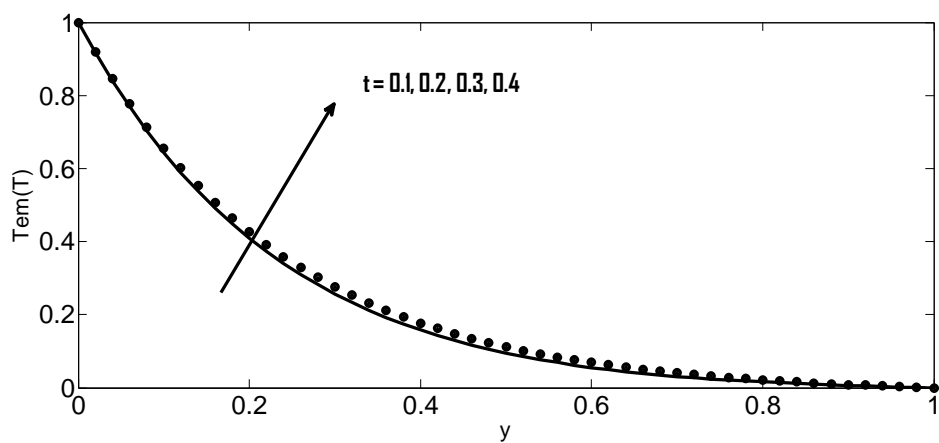
Fig.17. Effect of t on the temperature profiles
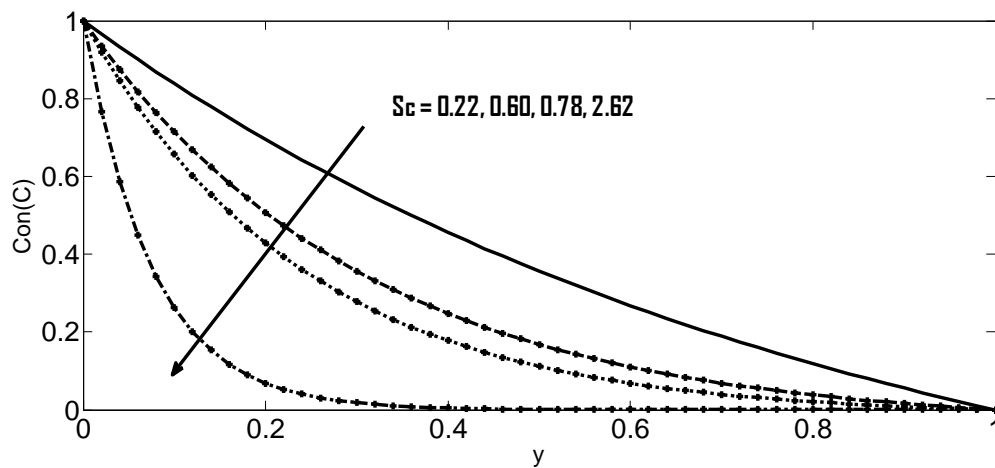
Fig.18. Effect of Sc on the concentration profiles
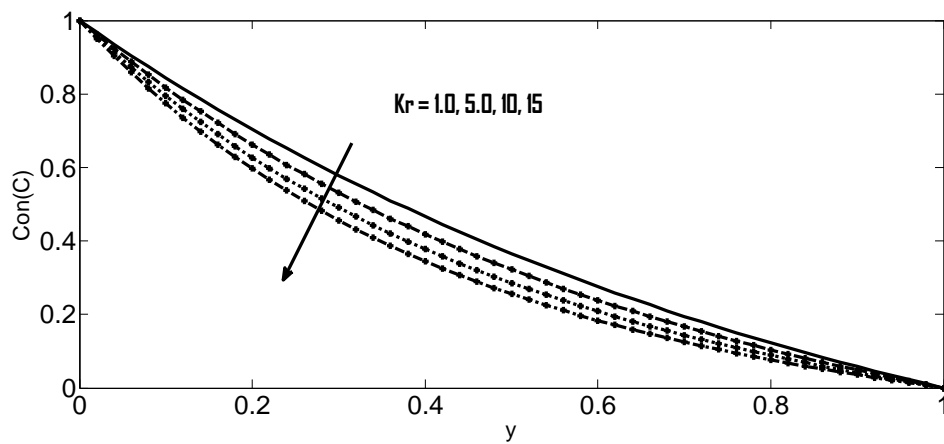
Fig.19. Effect of K_r on the concentration profiles
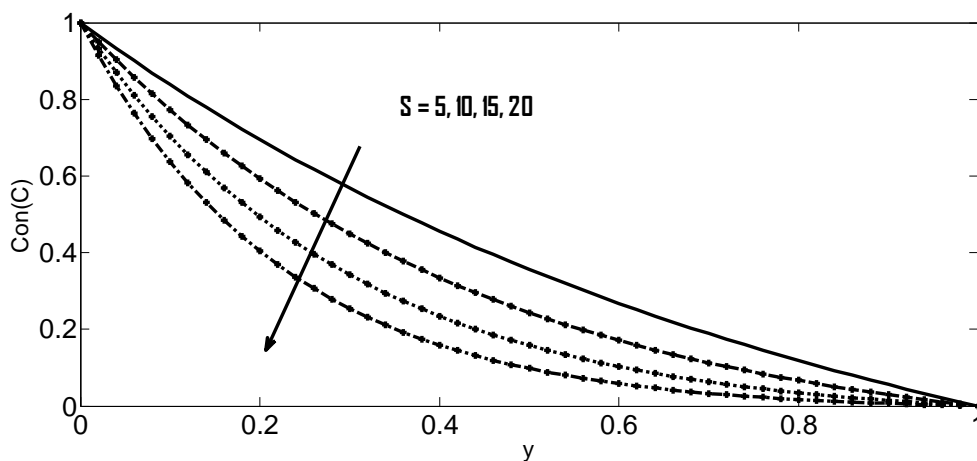
Fig.20. Effect of ($\gamma = S$) on the concentration profiles
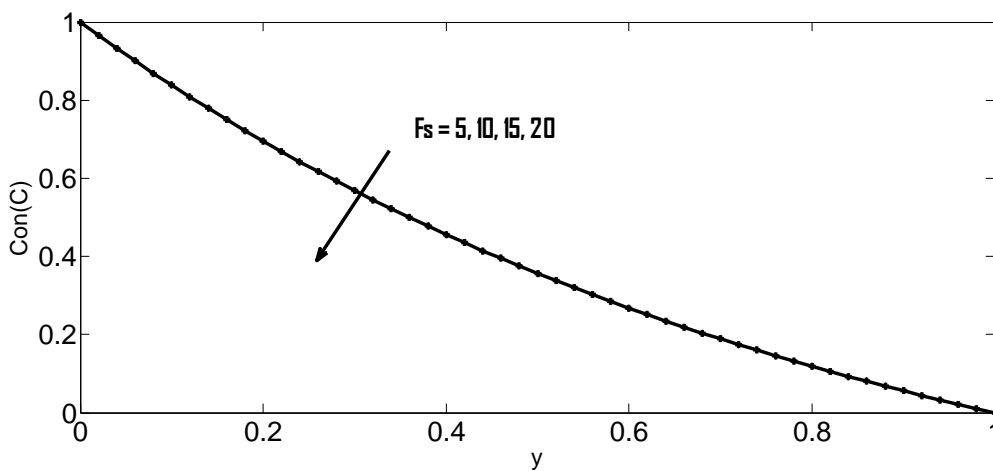
Fig.21. Effect of Fs on the concentration profiles
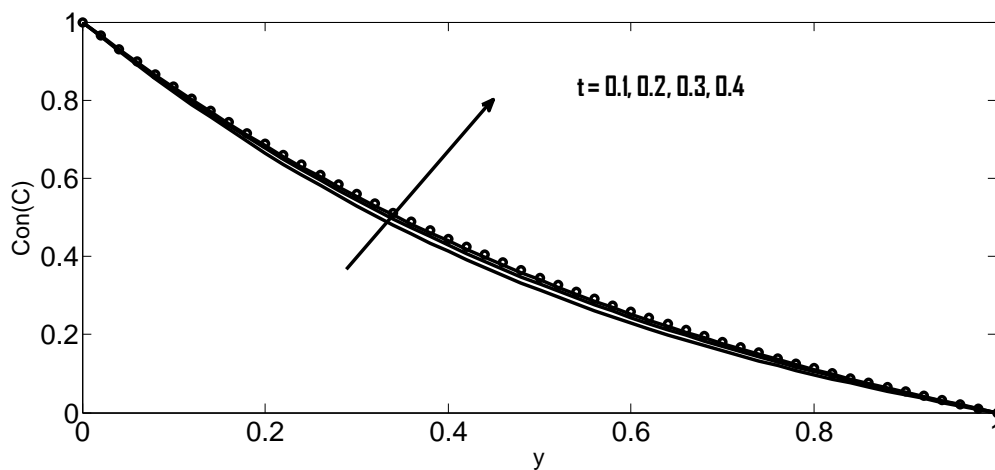
Fig.22. Effect of t on the concentration profiles
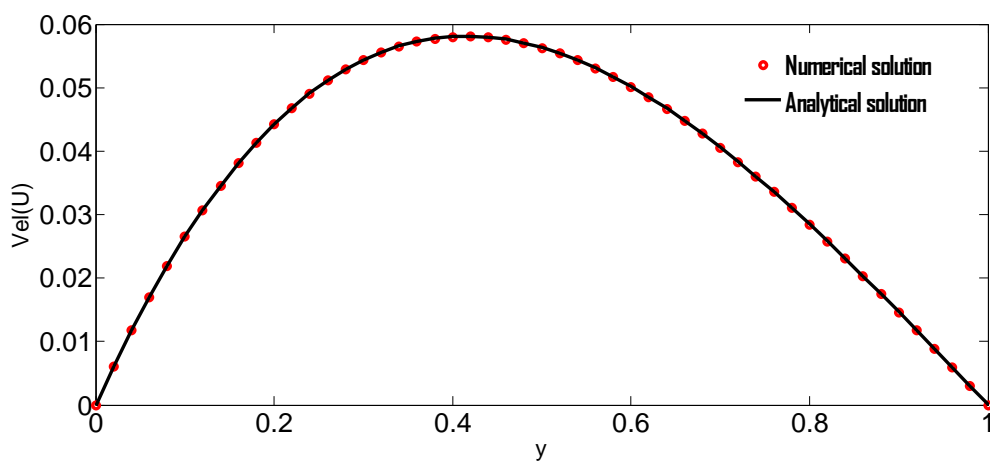
Fig.23. Comparison of numerical and analytical solutions for velocity profiles
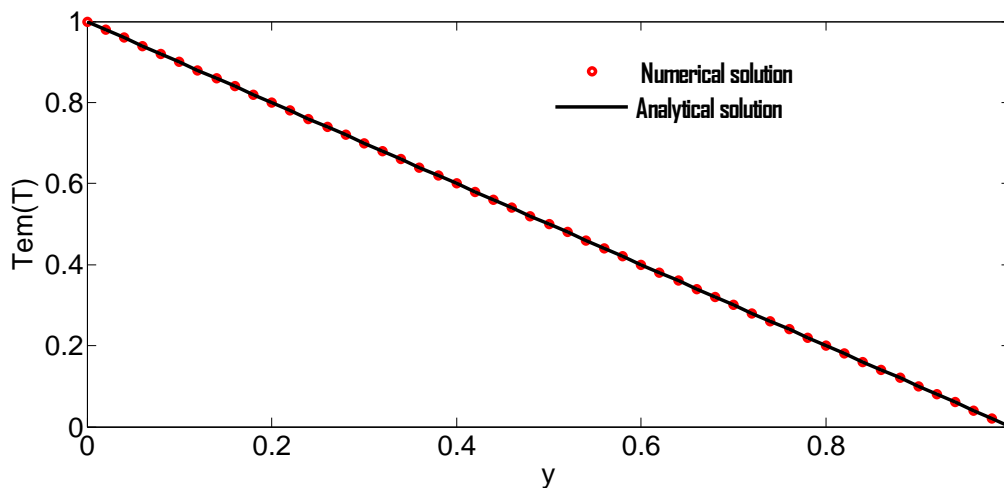
Fig.24. Comparison of numerical and analytical solutions for temperature profiles
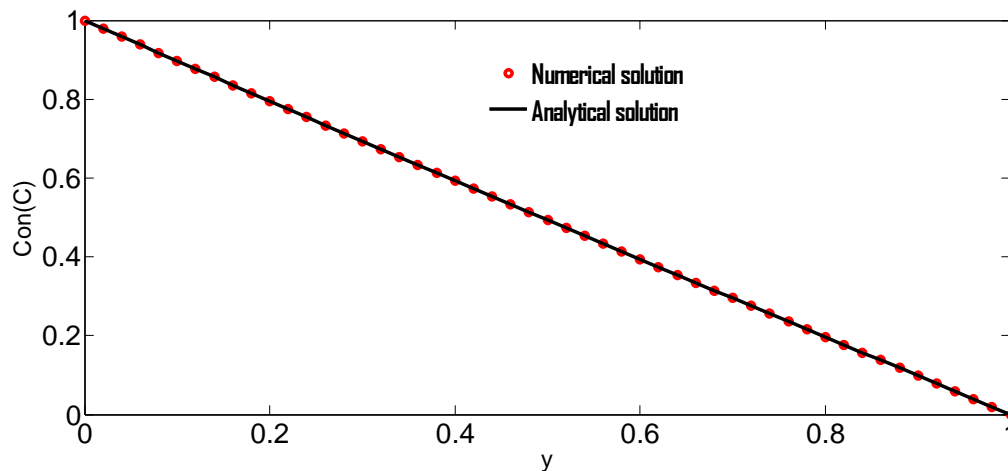
Fig.25. Comparison of numerical and analytical solutions for concentration profile**s**

Table 1 elucidates the effect of thermal conductivity parameter on skin friction and Nusselt number respectively. It is observed that an increase in λ causes a reduction in the skin friction coefficient for $(\Pr = 0.71, 7.0)$ respectively. Whereas heat transfer rate increase as expected with increase in λ and $\Pr$. The effects of various thermo physical parameters on Sherwood number are shown in Table 2. It is observed that the Sherwood number increases with an increase in Schmidt number and chemical reaction parameter respectively, but it is noticed that there is no significant change in the Sherwood number when the thermal Grashof number, thermal conductivity parameter and Darcy-Forchheimer parameter are increased.

Table 1: Skin friction (C_f) and Nusselt number (Nu) for different values of thermal conductivity ($/ = V$) and Prandtl number with $\gamma = 0.1, Gr = 0.5, Gc = 1, M = 1, K_r = 1, R = 0.1, Sc = 0.6, Fs = 5, Da = 0.5$.

λ	C_f $\Pr = 0.71$	C_f $\Pr = 7.0$	Nu $\Pr = 0.71$	Nu $\Pr = 7.0$
0	0.2820	0.2360	1.5656	5.1088
0.05	0.2826	0.2363	1.5276	4.9952
0.1	0.2832	0.2367	1.4908	4.8839
0.2	0.2843	0.2374	1.4207	4.6682
0.25	0.2848	0.2377	1.3872	4.5638
0.3	0.2854	0.2381	1.3547	4.4617

Table 2: Sherwood number (Sh) for different values of (Gr, Sc, K_r, λ, Fs) with $\gamma = 0.1, Gc = 1, M = 1, R = 0.1, Da = 0.5, \Pr = 0.71$.

Gr	Sc	K_r	λ	Fs	Sh
5	0.22	01	0.05	3.0	1.0835
10	0.22	01	0.05	3.0	1.0835
5	**0.60**	01	0.05	3.0	1.2802
5	0.22	**2.0**	0.05	3.0	1.1537
5	0.22	01	**0.1**	3.0	1.0835
5	0.22	01	0.05	**7.0**	1.0835

VI.   Conclusion

A finite difference solution of MHD free convective flow in a vertical channel with constant suction and thermal conductivity in a Darcy-Forchheimer porous medium has been analyzed both analytically and numerically. The resulting governing equations of the problem are non-dimensionalised, simplified and solved by Crank Nicolson type of implicit finite difference method. It reveals that the velocity increased due to increases in either of the Darcy parameter or thermal conductivity parameter and decreased as the magnetic parameter, Darcy-Forchheimer parameter, Prandtl number, and suction parameter were increased. An increased in the fluid temperature and the thermal boundary layer thickness is a function of an increased in thermal conductivity parameter and radiation parameter. In addition, the concentration decreased as either of the Schmidt number or

chemical reaction parameter or suction or Darcy-Forchheimer parameters was increased. The thermal conductivity and Prandtl number decreases the skin friction coefficient, whereas reverse trend is seen in the rate of heat transfer increasing with increase in thermal conductivity and Prandtl number. Also, the Schmidt number and chemical reaction parameter increases the Sherwood number. It is hoped that solutions presented in this work for various thermo physical effects will serve as a tool for understanding more general problems in heat and mass transfer in metallic materials processing and also in geophysical processes.

Acknowledgment

Nomenclature

C – Concentration

C_p – Specific heat at constant pressure

D - Mass diffusivity

g – Acceleration due to gravity

Gr – Grashof number

Gc – Solutal Grashof number

Nu – Nusselt number

Pr – Prandtl number

Sc – Schmidt number

R - Radiation parameter

K_r - Chemical reaction parameter

T – Temperature

C_f -Skin friction

Sh - Sherwood number

u, v – velocities in the x and y-direction respectively

x, y – Cartesian coordinates along the plate and normal to it respectively

B_0 - Magnetic field of constant strength

M – Magnetic field parameter

Da -Darcy number

Fs -Forchheimer number

Greek letters

β* - Coefficient of expansion with concentration

β - Coefficient of thermal expansion

ρ- Density of fluid

θ- Dimensionless temperature

υ- Kinematic viscosity

γ - suction parameter

λ - Variable thermal conductivity

σ - electrical conductivity of the fluid

References

[1]. M. Abdou, Effect of radiation with temperature dependent viscosity and thermal conductivity on unsteady stretching sheet through porous medium, Non-linear Analysis: Modeling and Control, 15(3), (2010), 257-270.
[2]. B. Carnahan, H. A. Luther and J. O. Wilkes, Applied numerical methods, John Wiley and Sons, New York, (1996).
[3]. T. C. Chiam. Heat transfer in a fluid with variable thermal conductivity over a linearly stretching sheet, Acta Mechanic, 129, (1998), 63-72.
[4]. P. Gitima, Effects of variable viscosity and thermal conductivity of micropolar fluid in a porous channel in presence of magnetic field, International Journal for Basic Sciences and Social Sciences, 1(3), (2012), 69-77.
[5]. M. A. Hossain, M. S. Munir and I. Pop, Natural convection with variable viscosity and thermal conductivity from a vertical wavy cone, International Journal of Thermal Sciences, 40, (2001), 437- 443.
[6]. D. B. Ingham and I. Pop, Transport phenomena in porous media, Elsevier, Oxford, UK. (2005).
[7]. R. Kandasamy, K. Perisamy and P. K. Sivagnana, Effects of chemical reaction, heat and mass transfer along a wedge with heat source and concentration in the presence of suction or injection, International Journal of Heat and Mass Transfer, 48, (2005,) 1388-1394.

[8].   N. Kishan, M. Srinivas, R. C. Srinivas, MHD effects on free convective heat and mass transfer in a doubly stratified non-Darcy porous medium, International Journal of Engineering Sciences and Technology, 3(12), (2011), 8307-8324.

[9].   F. C. Lai, Coupled heat and mass transfer by mixed convection from a vertical plate in a saturated porous medium, International Communication Heat and Mass Transfer, 18, (1991), 93-106.

[10].   Mahdy and Chamkha, Chemical reaction and viscous dissipation effects on Darcy-Forchheimer model convection in a fluid saturated media, International Journal of Numerical Methods for Heat and Mass Transfer Fluid Flow, 20(8), (2010), 924-940.

[11].   F. Mohammad, O. Masatiro, S. Abdus and A. Mohamud, Similarity solution for MHD flow through vertical porous plate with suction, Journal of Computational and Applied Mechanics, 6(1), (2005), 15-25.

[12].   D. A. Nield and A. Bejan, Convection in porous media, third edition, Springer, New York, (2006).

[13].   G. Patowary and K. Dusmata, Effects of variable viscosity and thermal conductivity of micropolar fluid past a continuously moving plate with suction or injection in presence of magnetic field, International Journal of Mathematics Trend and Technology, 2(2), (2011), 32-36.

[14].   S. Rawat, R. Bhargava and B. O. Anwar, A finite element study of the transport phenomena MHD micropolar flow in a Darcy-Forchheimer porous medium, Proceedings of the World Congress on Engineering and Computer Science, Oct 24-26, (2007).

[15].   M. A. Sattar, Free and forced convection boundary layer flow through a porous medium with large suction, International Journal of Research in Energy Research, 17, (1993), 1-7.

[16].   N. H. Saied and I. Pop, Natural convection from discrete heater in a square cavity filled with a porous medium, Journal of Porous Media, 8(1), (2005), 55-63.

[17].   A. M. Salem, Coupled heat and mass transfer in Darcy-Forchheimer mixed convection from a vertical flat plate embedded in a fluid-saturated porous medium under the effects of radiation and viscous dissipation, Journal of the Korean Physical Society, 48(3), (2006), 409-413.

[18].   M. A. Seddek and F. A. Salema, The effects of temperature dependent viscosity and thermal conductivity on unsteady MHD convective heat transfer past a semi-infinite vertical porous moving plate with variable suction, Computational Material Science, 40(2), (2007), 186-192.

[19].   P. R. Sharma and G. Singh, Effects of variable thermal conductivity and heat source/sink on MHD flow near a stagnation point on linearly stretching sheet, Journal of Applied Fluid Mechanics, 2(1), (2009), 13-21.

[20].   I. J. Uwanta and S. Murtala, Heat and Mass Transfer flow past an infinite vertical plate with variable thermal conductivity, International Journal of Applied Information System, 6(1), (2013), 16-24.

[21].   K. Vafai and C. L. Tien, Boundary and inertia effects on flow and heat transfer in a porous media, International Journal of Heat Mass Transfer, 24 (1981) 195-203.